Mon. Not. R. Astron. Soc. **264,** 579–586 (1993)

The absolute proper motion and Galactic orbit of M3

R.-D. Scholz,[1] M. Odenkirchen[2] and M. J. Irwin[3]

[1] *WIP-Projekt Astrometrie bei der Universität Potsdam An der Sternwarte 16, O-1590 Potsdam, Germany*
[2] *Sternwarte der Universität Bonn Auf dem Hügel 71, W-5300 Bonn 1, Germany*
[3] *Royal Greenwich Observatory, Madingley Road, Cambridge CB3 0EZ*

Accepted 1993 March 23. Received 1993 March 15; in original form 1992 December 23

ABSTRACT

The combination of Schmidt plates and an automatic measuring machine provides a powerful method for investigating the proper motions of both the Galactic halo globular clusters and the nearby Galactic dwarf spheroidal satellites. We describe the first direct measurement of the absolute proper motion of a Galactic globular cluster with respect to a large number of background galaxies. Five pairs of Tautenburg Schmidt plates centred on the cluster M3, with epoch differences from 20 to 23 yr, were scanned using the automatic plate measuring facility in Cambridge. The proper motion determination was based on a stepwise regression method with generalized third-order polynomials and used between 1200 and 2200 galaxies for each pair of plates to define an inertial reference frame. The mean absolute proper motion of the cluster is found to be $\mu_x = -0.31 \pm 0.02$ and $\mu_y = -0.23 \pm 0.04$ arcsec $(100\ \mathrm{yr})^{-1}$. Using this proper motion, together with the known radial velocity and distance to M3, we can infer the orbital parameters of the globular cluster in a Galactocentric inertial system.

Key words: astrometry – globular clusters: individual: M3 – Galaxy: kinematics and dynamics.

1 INTRODUCTION

Our present knowledge of the kinematics of the Galactic globular cluster system is mainly based on radial velocity studies. The key to further progress lies in the determination of absolute proper motions. Webbink (1988) reviewed the efforts in both directions and encouraged new attempts to obtain absolute proper motions of globular clusters directly with respect to background galaxies and quasars.

Proper motions of numerous globular clusters have been investigated by Cudworth and coworkers by measuring the relative motion of cluster stars with respect to field stars. This required various assumptions concerning the direction of the solar apex and the secular parallaxes of the chosen field stars around each cluster. Not only were the results affected by the choice of solar apex and motion, but they were also afflicted by large errors due to the small number of field stars used (~ 50) and their inherent proper motion dispersion (e.g. Cudworth 1979). Although a very high accuracy [± 0.02 arcsec $(100\ \mathrm{yr})^{-1}$] in the relative proper motion of the cluster stars was achieved, the uncertainty in the absolute proper motion of the whole cluster remained of the order of 0.1–0.4 arcsec $(100\ \mathrm{yr})^{-1}$. In an attempt to circumvent this problem, Brosche, Geffert & Ninkovic (1983) and Brosche et al. (1985) used Lick stars with known absolute proper motions as reference stars to connect globular cluster motions to an extragalactic reference frame, while Tucholke (1992a,b) derived the proper motion of globular clusters relative to the background of the Small Magellanic Cloud (SMC).

In this paper we describe the first direct measurement of the absolute proper motions of a globular cluster with respect to a large number (~ 2000) of background galaxies. The big Schmidt telescope (134/200/400) of the Karl-Schwarzschild-Observatorium, Tautenburg, near Jena has been taking photographic plates of some globular clusters since the early 1960s. With a 25-yr baseline it is now possible to use this material to study the proper motions of these globular clusters. Five pairs of Tautenburg Schmidt plates in the field with the globular cluster M3 were processed on the automatic plate measuring (APM) facility in Cambridge. The APM facility has already been extensively used for astrometric work using UK Schmidt and Palomar Schmidt photographic plates (Kibblewhite et al. 1982; Kibblewhite et al. 1984; Evans 1988).

With an improvement of the accuracy in the absolute proper motion of M3 by a factor of 10 compared with the previous attempt of Cudworth (1979), we are able to determine the orbital parameters of the globular cluster. The residual variation of this orbit due to the remaining uncertainty not only in the proper motion components but also in the other initial parameters is found to be relatively small.

2 OBSERVATIONS AND MEASUREMENTS

The Tautenburg Schmidt telescope, with a 2-m mirror, a 1.34-m correction plate and a focal length of 4 m, has a plate scale of 51.4 arcsec mm^{-1}. With a useful plate size of 24 cm, each plate covers some $3.^{\circ}3 \times 3.^{\circ}3$ of sky, providing sufficient background galaxies to define an absolute inertial reference frame. Until recently, astrometric measurements of Tautenburg Schmidt plates were carried out by semi-automated measuring machines such as a Zeiss ASCORECORD. Because of their relatively slow measuring rate the numbers of reference galaxies and stars that could be included were severely restricted (Schilbach 1982; Scholz & Rybka 1988).

Among the fields for which first-epoch plates taken between 1960 and 1970 are available (see Scholz & Hirte 1991) are several centred on the globular cluster M3. Five plate pairs with epoch differences between 20 and 23 yr (see Table 1) were measured on the APM in order to extract optimally all the information available on the plates. All plates were measured by placing them on an optically flat 6 mm thick glass plate using nonane (a liquid of comparable refractive index to glass) to stick the plate on to the glass surface. This procedure ensures that the plates are orthogonal to the measuring beam over the whole area, removes the need for autofocusing of the laser spot, and prevents fringes occurring from the coherent illuminating laser light. The plates were orientated using reference stars from the PPM catalogue (Röser & Bastian 1988), so that all x and y proper motions listed below correspond to $\mu_\alpha \cos\delta$ and μ_δ respectively.

The total available field per plate is 10.5 deg^2 and the plate pair overlaps are given in Table 1. The variation in overlap area was due partly to the calibration wedge in the north-eastern corner of all the second-epoch plates and partly to a shift of the field centre in the case of plates 6226 and 6232. In all cases the cluster field centre is within ± 7 arcmin of the centre of the overlap zone, giving a good distribution of field stars and reference galaxies about the cluster. Images within about 2 arcmin of the cluster centre were too crowded to be reliably measured and were excluded from subsequent processing.

All plates were taken through a blue GG13 filter with exposure times between 20 and 30 min. An internal magnitude calibration as described by Bunclark & Irwin (1983) was applied. In a previous study (Scholz & Schmidt 1992), the internally calibrated APM magnitudes, which are linearly related to photoelectric magnitudes, were converted into B magnitudes using the photographic photometry of Bronkalla (1972) on the Tautenburg plates 2175 and 2176 with respect to some photoelectric standards. The accuracy of our stellar magnitudes is estimated to be about ± 0.1 mag.

One of the plates (6226) was measured twice, with a time interval between measurements of several days, to assess the repeatability of the APM measurements of Tautenburg Schmidt plates. The positional repeatability for different magnitude classes and types of object (stars and galaxies) is shown in Fig. 1. We defer discussion of systematic errors in plate measurement to the next section, but it is clear from Fig. 1 that the random errors for repeat measurements are less than 0.5 μm for stars and less than 1 μm for galaxies, over a wide range of magnitudes.

Further assessment of the likely plate-to-plate positional errors was made by pairing up some other Tautenburg plates taken at the same epoch and measured with the APM (Scholz 1990). For these plate pairs a positional accuracy of between 1 and 2 μm (0.05 and 0.10 arcsec) was achieved for stars in the magnitude range $B = 10$–17, indicating that the main source of error in any astrometric comparison will be governed by the plate material, not the APM. For fainter objects, the plate-to-plate errors are completely dominated by random errors in the recording process: Poisson and photographic grain noise (see for example Irwin 1985). For $B = 19$, therefore, the stellar positional accuracy was 3 μm, whilst for galaxies it rose to 5 μm and higher. Scholz (1990) also looked for both field- and magnitude-dependent positional errors. Whereas coma-like effects could not be found, magnitude-dependent systematic shifts of up to a few μm were apparent for some of the plate pairs. This appears to be caused by a combination of asymmetric image profiles and photographic saturation. Basically, in good seeing, some 3–4 mag above the plate limit all the stellar images begin to saturate. Any centring algorithm, whether it be a centre of gravity method or even a profile-fitting method, sees a fraction of the image profile that varies as a function of magnitude. If the underlying profile is asymmetric the

Table 1. Details of the plates centred on M3.

Plate No. 1st epoch 2nd epoch	Epoch	Overlap zone [sq. degrees]	No. of galax.	Error of x solution y solution [μm]	Absolute p.m. error in x in y [arcsec/100yr]	Weight of the pair
2176	1966.2	10.0	2163	7.2	0.035	1.4
7000	1989.2			6.7	0.032	
2175	1966.2	10.0	1947	7.7	0.039	1.3
6999	1989.2			7.7	0.039	
2873	1969.3	10.0	1230	9.0	0.066	0.7
7002	1989.2			9.2	0.068	
2167	1966.2	9.2	1761	8.3	0.050	0.9
6226	1986.4			8.4	0.051	
2174	1966.2	9.2	1383	10.5	0.072	0.7
6232	1986.4			9.7	0.066	

Notes: all exposure times were between 20 and 30 min; column 5 is the average plate-to-plate rms error for the galaxies.

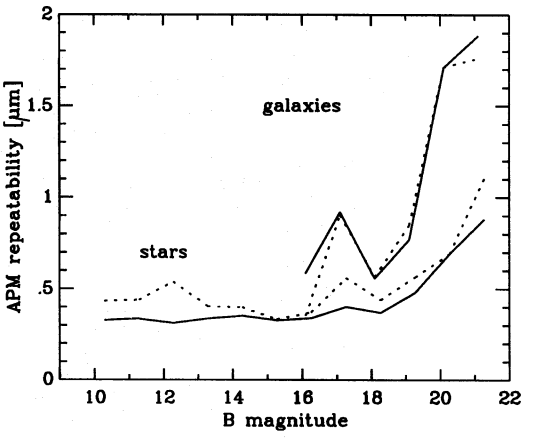

Figure 1. Repeatability of APM measurements on Tautenburg plate 6226. The solid lines represent the repeatability of the x-coordinates, the dotted lines the repeatability of the y-coordinates.

derived centre will depend in a subtle way on how much of the image is lost to saturation. Fortunately, the vast majority of stars in the cluster are not saturated, and the same is true of the background galaxies that are used for an inertial reference frame. Indeed, no statistically significant magnitude effect was seen in the galaxy measurements. So, providing that the brightest cluster stars are not used in determining the cluster proper motion, this magnitude dependence is not a problem.

3 DETERMINATION OF THE ABSOLUTE PROPER MOTION

3.1 Plate matching and selection of objects

For the plate matching of all 10 plates, we used the deepest first-epoch plate as the reference plate. The plate matching consists of pairing up objects between the reference plate and the comparison plates using several passes of ever-decreasing search radius, starting with bright objects and large search radii (up to several mm) and finally iterating down to faint objects within a target search radius of 30 μm. With a 20-yr baseline this corresponds to a proper motion of 7.5 arcsec $(100\ \mathrm{yr})^{-1}$, so that only very high proper motion objects were excluded. Only astrometric criteria were used in the matching, since with a final search radius of 30 μm the probability of generating a spurious mismatch is negligible (<0.01 per cent at these number densities).

The measured objects were classified into stars, non-stellar objects, noise images and merged objects using the standard APM software. In order to exclude objects that were unreliably recorded or measured (due to, say, excessive image crowding, dirt or emulsion defects) only those images classified as stars on all plates or as galaxies on at least the two deepest plates were used in subsequent analysis. In accordance with the number density of these stars obtained from our measurements, we assumed a cluster radius of 16 arcmin. At this distance from the cluster centre the number density of stars with $17<B<20.3$ is still more than twice that in the outer field (see Fig. 2). All stars inside this radius were considered as cluster stars. The stellar number density increases rapidly towards the cluster centre, but due to the crowding it appears to decrease again in the very central region. The number density of the objects with $17<B<20.3$ classified as non-stellar on at least the two deepest plates is also shown in Fig. 2. The reference galaxies were selected only outside a radius of 16 arcmin because of possible overlapping images of cluster stars masquerading as galaxies.

The faintest stars and galaxies ($B>20.3$) were not used, both because of their rapidly increasing positional errors and because of the uncertainty in the image classification of galaxies near the plate limit. Bright galaxies ($B<17$) were not used because of the possible misclassification of bright stars and double stars (e.g. Schilbach & Scholz 1992). Finally, we decided not to use the bright cluster stars ($B<17$) because, even allowing for the extra information present in the membership probabilities of these stars obtained by Cudworth (1979), possible magnitude-dependent systematic errors could begin to dominate the mean cluster motion. For example, systematic errors of 1 μm for brighter stars, as found by Schilbach & Scholz (1992) in a comparison of another two Tautenburg plates measured with the APM,

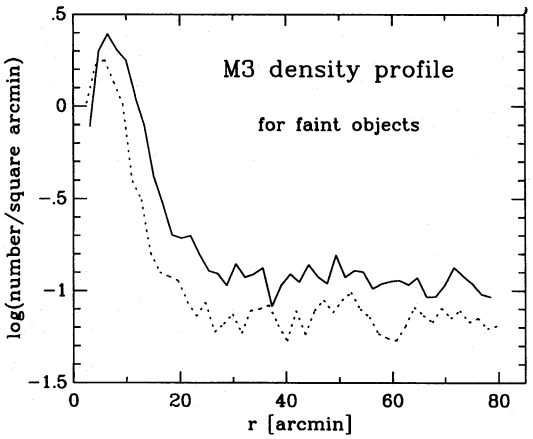

Figure 2. Number density as a function of cluster radius. The solid line represents objects with $17<B<20.3$ classified on all 10 plates as stars; and the dotted line objects in the same magnitude interval classified as galaxies on the deepest two plates.

would contribute a fictitious 0.025 arcsec $(100\ \mathrm{yr})^{-1}$ proper motion to the cluster, if they contributed ~10 per cent of the cluster stars.

3.2 Plate-to-plate solution and systematic error removal

The global plate-to-plate transform models for each pair of plates were obtained with different samples of reference galaxies using third-order polynomials and the method of stepwise regression described in Hirte et al. (1990). Only coordinate-dependent terms were included, and only statistically significant terms are retained. Magnitude-dependent terms were omitted because the magnitude interval for the objects used had already been restricted. The reference galaxies were defined by the requirements that on the two deepest plates they be classified as galaxies, that they lie outside a radius of 16 arcmin from the cluster centre, and that they be in the interval from $B=17$ to 1 mag above the plate limit to ensure reliable classification. The number of galaxies (see Table 1) depends on the limiting magnitudes of the plates in a pair, and consequently on the different quality of the images, which influences the matching with the reference plate. The overall limiting magnitude was $B=21.3$. An estimate of the quality of the plate pairs can be obtained directly by dividing the unit weight error of the plate-to-plate solution by the epoch difference and the square root of the number of galaxies used in the solution. This formal error in defining an inertial reference frame in the field centre where the cluster is situated was used to compute weights for the plate pairs (Table 1). The different weights were mainly due to the lower plate limit of one first- and one second-epoch plate.

Using these weights, we obtained mean absolute proper motions from five pairs of plates. Binning the whole field into 10×10 subareas and computing the mean motion of all stars in each subarea, we obtained a first illustration of the difference in the proper motions of the field stars and the cluster (see Fig. 3). Note that there were no proper motion data in the upper right corner of the field due to the calibration wedge on all second-epoch plates. The mean absolute proper

motion is nearly constant all over the field (showing the reflex motion of the Sun), whereas in the field centre where the cluster is situated the movement is in the same direction but is clearly slower. Note that no systematic error removal was used at this stage.

Kibblewhite et al. (1982) and Evans (1988) described another astrometric reduction method for the APM measurements, whereby any systematic errors on scales of 1–2 cm are detected and then removed after first applying a linear plate-to-plate solution. Likewise, any systematic errors caused by column-scanning the plates in stripes 2 mm wide are also estimated and removed. The general idea is to model locally any systematic errors, whatever the cause (e.g. measuring machine, differential field distortion, plate emulsion non-elasticity, etc.), and simply subtract them. Although this approach works well for studies of Galactic structure (the original motivation), in which the mean proper motion of stars over this size of field is essentially independent of position, for analysing the proper motion of a globular cluster, which itself only covers a few cm of plate, a modification of this method is required. Since, however, all the plates were taken using the same telescope set-up and had relatively short exposure times, high-order plate-to-plate corrections (or rubber-membrane-type corrections) were found not to be needed.

Consequently, we looked for systematic effects in the x and y proper motions dependent on the x and y position obtained from the global polynomial method. Periodic errors such as the so-called '2-cm wobble' (Evans 1988; Schilbach & Scholz 1992) may not change the mean proper motion of the stars uniformly distributed over the whole field, but they have to be considered in the case of a globular cluster with rather different number densities as a function of the coordinates. These 'global' systematic effects, ~ 3 μm peak-to-peak, are a function of the design of the x–y table and are repeatable in an absolute sense. Fig. 4 shows an example of the main periodic error for one of the plate pairs. This is the dependence of the y proper motion on the x-coordinate. The two lines represent this function for the faint field and cluster stars. For the correction of the cluster proper motion in both x and y we assumed a constant proper motion for the field stars outside a given cluster radius and another constant proper motion for the cluster stars inside this radius (cf. Fig. 3). We can also assume equal systematic errors of the x and y proper motions as a function of the x and y position for both the cluster and the field stars. Binning the cluster and field star proper motions along the x and y axes, the corrected mean cluster proper motion was therefore obtained by summing the mean field star proper motion and the mean difference of corresponding bins.

There is also a small (~ 1 μm) systematic error of period 2 mm, which is a result of measuring the plate in 2-mm-wide strips using a flying laser spot. This is simply caused by the variation of the y-table position of the laser beam within a 2-mm lane from one end of the beam scan to the other, due to the finite traveltime of the beam sweep and the fact that the table moves continuously in y during a lane scan. Although this error averages out over the several-cm region occupied by the cluster (and field stars), it was also removed prior to estimating the final cluster proper motion with respect to the background galaxies (see Evans 1988 for more details).

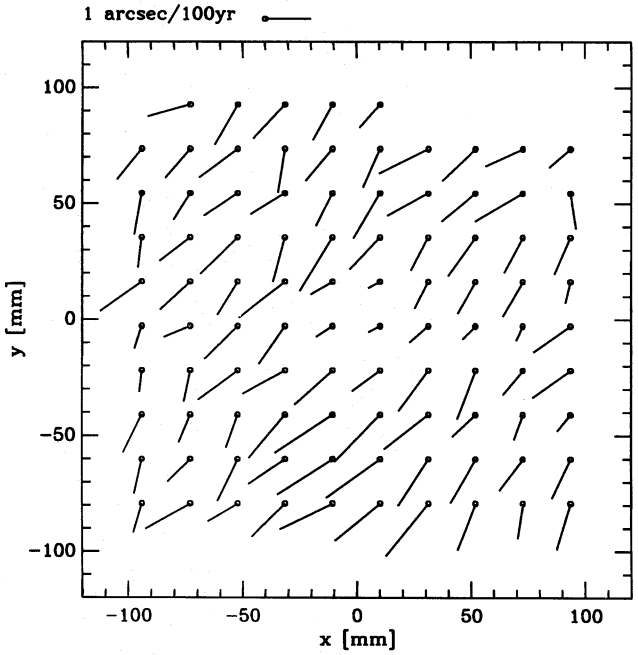

Figure 3. Uncorrected mean absolute proper motions from five pairs of plates averaged in subareas.

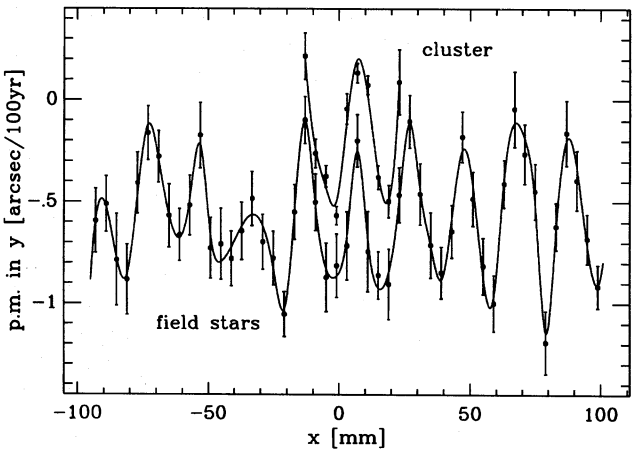

Figure 4. The dependence of the '2-cm wobble', which is typical of all pairs of plates, in the y proper motions of faint field stars and cluster stars on the x-position. Error bars on the mean proper motions after binning along the x-axis and cubic spline interpolations are also shown. The correlations of the y proper motions with x and of the x proper motions with x and y are not so strong. The corrected cluster proper motions were obtained separately for each pair of plates, as the mean proper motion of the field stars plus the mean difference between the data on cluster stars and the data on field stars in the corresponding bins.

3.3 Internal proper motion accuracy and comparison with previous results

The results of the determination of the absolute proper motion of the cluster are listed in Table 2. The data obtained for the five different pairs of plates are shown in Fig. 5. Obviously, the x and y values of the absolute proper motions that were corrected for the systematic errors as

Table 2. Mean absolute proper motion of M3.

	Mean absolute p.m. in x [arcsec/100yr]	Mean absolute p.m. in y [arcsec/100yr]
uncorrected	−0.28±0.04	−0.18±0.06
corrected	−0.31±0.02	−0.23±0.04

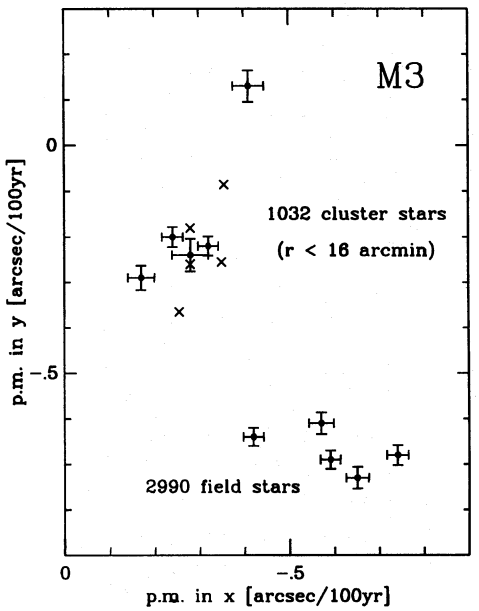

Figure 5. Absolute proper motions from five pairs of plates. For each pair of plates the mean absolute proper motions of the cluster stars and of the field stars (both in the magnitude range $17 < B < 20.3$), and their dispersions, are shown. The crosses mark the results of the correction for systematic effects, which are partly due to the APM machine.

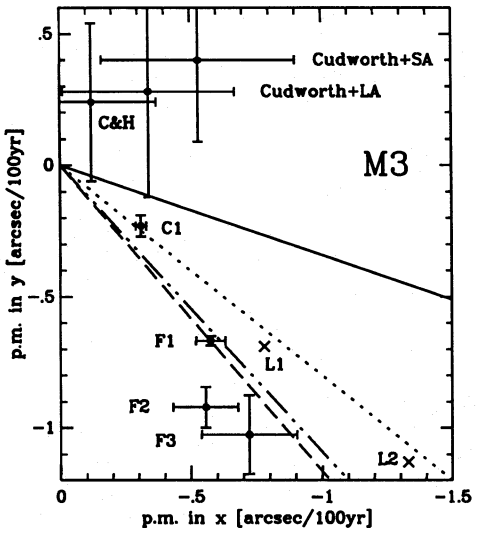

Figure 6. Mean absolute proper motions of cluster stars and field stars in comparison to the results of Cudworth (1979), who used standard apex (SA) or Lick apex (LA). The result of a re-reduction of the absolute M3 proper motion by Cudworth & Hanson (1993), shown in the figure as C&H, is still quite uncertain. Points corresponding to field and cluster stars together with the error bars on the mean proper motions from five pairs of plates are marked. C1 is the corrected cluster motion for 1032 cluster stars with $17 < B < 20.3$; F1 is the mean proper motion for 2990 field stars with corresponding magnitudes; F2 is the mean proper motion for 1121 field stars with $14 < B < 17$; and F3 is the mean proper motion for 220 field stars with $B < 14$. The points labelled L1 and L2 are Lick proper motion measurements for about 50 faint and bright stars respectively taken from Klemola & Vasilevskis (1971). The solid line represents standard antapex, the dashed line solar antapex with respect to globular clusters, the dot–dashed line old Lick solar antapex, and the dotted line new Lick solar antapex.

described previously are in better agreement than the uncorrected ones. The error bars in Fig. 5 represent the dispersion of the mean cluster motion and of the mean field star proper motion separately for each pair of plates.

A comparison of the results with those of Cudworth (1979) and with the recently published reduction of Cudworth & Hanson (1993) is shown in Fig. 6. Here our error bars represent the mean error of the weighted mean from five pairs of plates. Also shown in Fig. 6 are the directions of the standard antapex, the old Lick antapex (Klemola & Vasilevskis 1971), the new Lick antapex (Hanson 1987) and the antapex for the Galactic globular cluster system taken from Mihalas & Binney (1981). There is a significant difference between the field and cluster proper motions. As expected, there is a general trend for the proper motions of the field stars to increase with the brightness of the samples. We also find a slightly different direction for the proper motion vector compared with the Lick results, although it is worth noting that the Lick sample only contains ~ 50 stars in each bin.

4 DETERMINATION OF GALACTIC ORBIT

Proper motions measured in an extragalactic reference system offer a direct approach to the space motion of the cluster. To yield a complete set of six space and velocity components in a Galactocentric inertial system, one must combine proper motions with measurements of the heliocentric distance, position and radial velocity of the cluster and the location and motion of the Sun with respect to the Galactic Centre. Using the data given in Tables 3 and 4 and the method of Johnson & Soderblom (1987) we derived for M3 the space and velocity components shown in Table 5.

Together with any force field or potential that models the interaction of the cluster with the rest of the Galaxy, these components uniquely determine the orbit of the cluster in space. The orbit of M3 presented here is based on the three-component Galactic potential of Allen & Martos (1986) and on methods described in detail by Odenkirchen & Brosche (1992). Conventionally, the orbit was calculated over an interval of 10 Gyr backwards in time. However, for reasons of clarity Figs 7 and 8 refer to a shorter time interval. The derived orbital parameters of M3 are given in Table 6. A precise definition of the orbital quantities can be found in the notes to Table 3.

Fig. 7 shows a picture of the motion in the meridional plane, i.e. the plane spanned by the two cylindrical coordinates ρ, z. According to the fixed values of the two constants of motion E and J_z the cluster would be allowed to move in the interior of the dashed curve. With a rather low value of J_z

Table 3. Data from observations on M3.

α (1950) h	m	δ (1950) °	'	D [kpc]	v_r [km/s]	$\mu_\alpha \cos\delta$ [arcsec/100yr]	μ_δ
13	39.9	28	38	9.5±1.0	-146.9±0.5	-0.31±0.02	-0.23±0.04

Notes: D according to CMD of Paez (1990) and others; v_r according to Gunn & Griffin (1979).
Definition of symbols in Tables 3–7: D: distance of the object from the observer; v_r: radial velocity; x, y, z: space coordinates in a right-handed Galactocentric Cartesian coordinate system with z pointing to the Galactic North Pole and x opposite to the Sun; U, V, W: corresponding velocity components; U_{sun}, etc: peculiar motion components of the Sun in Local Standard of Rest; v_{LSR}: Galactic rotation velocity of Local Standard of Rest; R: distance from Galactic Centre; ρ: projected distance on the Galactic plane; $q_{min,max}$: minimum and maximum values of quantity q during 10 Gyr; $\bar{q}$: time average of q in 10 Gyr; Δq: maximum deviation of q and $\bar{q}$ in 10 Gyr; e: eccentricity defined as $(R_{max}-R_{min})/(R_{max}+R_{min})$; v: absolute value of velocity; v_φ: cylindrical φ-component of velocity vector; T: period of one revolution around the z-axis; n_U: number of revolutions in 10 Gyr; J: absolute value of angular momentum; J_z: z-component of the angular momentum vector; i: inclination of the orbital plane (the angle between the J-vector and the z-axis); n_ρ: number of rotations of the J-vector around the z-axis; E: total orbital energy.

Table 4. The estimated location and motion of the Sun in the Galactocentric inertial frame.

x_{sun}	y_{sun} [kpc]	z_{sun}	U_{sun}	V_{sun} [km/s]	W_{sun}	v_{LSR} [km/s]
-8.0±0.5	0.0	0.0	10.0±1.0	15.0±3.0	7.5±0.5	225±20

Table 5. Derived space and velocity components for M3.

x	y [kpc]	z	U	V [km/s]	W
-6.6±0.5	1.3±0.1	9.3±1.0	-53±14	54±31	-108± 4

the cluster could be expected to pass very close to the Galactic Centre. In fact, the meridional orbit remains within a much smaller area at distances between 5.1 and 12.3 kpc from the Centre, revealing the character of a box orbit: it runs across a strongly wound rectangular box similar to a Lissajous figure with approximate periodicity (note the reflection in the uppermost corner of the box). With increasing integration time the box and also its corresponding toroidal volume in space are filled up.

In Fig. 8 the orbit is shown during the same time interval but projected on to the Galactic plane. This figure reveals that the motion in space consists of rapidly precessing ellipses with oscillating eccentricity. Due to the negative value of J_z the cluster rotates around the z-axis clockwise with a mean period of 0.3 Gyr corresponding to 33.6 revolutions around the Centre in 10 Gyr. Frequency distributions of values for the orbital parameters R, v and v_φ based on the full interval of 10 Gyr are given in Fig. 9. Since motion becomes slower with increasing distance, a tendency for higher frequencies towards the upper end of the R distribution and the lower ends of the v and v_φ distributions is found.

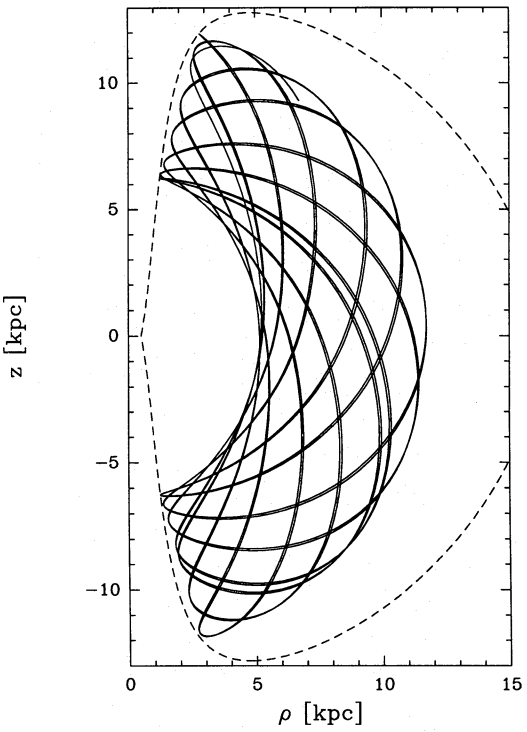

Figure 7. Meridional section of the orbit of M3 in the time interval (−4; 0) Gyr.

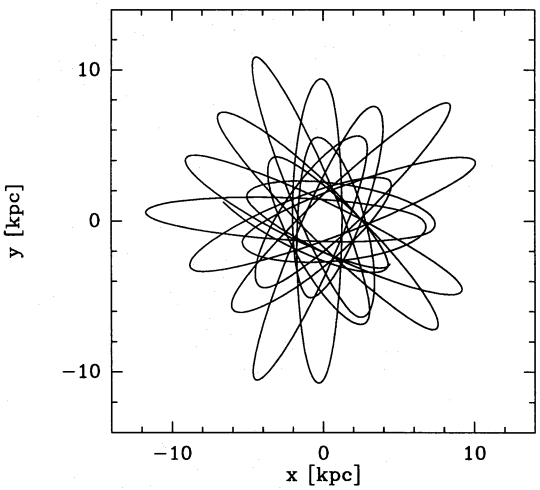

Figure 8. The orbit of M3 in the time interval (−4; 0) Gyr projected on to the Galactic plane.

v_φ remains below 100 km s^{-1} in absolute value for more than 80 per cent of the time. The present values of these parameters agree with the range of high probability (cf. Table 6). This may indicate consistency between observation and the orbit calculation for M3. From analysis of the behaviour of the angular momentum vector it follows that the orbital plane is subject to a small secular rotation around the z-axis while its inclination remains nearly constant with time. Mean values and extrema of the parameters mentioned above are documented in Table 6 together with a precise definition.

Table 6. Orbital parameters in the standard time interval for M3.

a) Geometry of the orbit

R_{min}	R_{max}	$\overline{R}$	$R(t=0)$	e	z_{min}	z_{max}
	[kpc]				[kpc]	
5.1	12.3	9.4	11.5	0.39	-12.0	12.0

b) Absolute value of velocity

v_{min}	v_{max}	$\overline{v}$	$v(t=0)$
		[km/s]	
104	331	186	132

c) Rotation around z-axis

$v_{\varphi,min}$	$v_{\varphi,max}$	$\overline{v}_{\varphi}$	$v_{\varphi}(t=0)$	$\overline{T}$	n_U
	[km/s]			[Gyr]	
-237	-25	-66	-43	0.30	33.6

d) Angular momentum and inclination of the orbit

$\overline{J}$	$\Delta J/\overline{J}$	$\overline{i}$	Δi	n_P
[kpc·km/s]		[degree]		
1516	$^{+29}_{-16}$%	101.2	$^{+2.0}_{-2.7}$	1.3

e) Constants of motion

J_z	E
[kpc·km/s]	[km^2/s^2]
-290	-116900

Table 7. Variation of the orbital parameters with the initial values for M3.

initial values	$\overline{T}$ [Gyr]	n_U	R_{min}	R_{max} [kpc]	$\overline{R}$	e	z_{min}	z_{max} [kpc]
mean	0.30	33.6	5.1	12.3	9.4	0.39	-12.0	12.0
+var1	0.29	35.0	4.1	12.3	9.1	0.50	-12.3	12.3
-var1	0.32	31.1	6.7	12.4	9.9	0.30	-11.7	11.7
+var2	0.31	32.2	5.9	12.5	9.7	0.36	-12.3	12.3
-var2	0.29	34.3	4.6	12.1	9.1	0.45	-11.7	11.7

We have included in Tables 3 and 4 an estimation of the possible errors in the observational data. These errors lead to some uncertainty in the initial values and this again must produce some variations in the orbit and its characteristic parameters. Table 5 gives errors of the initial values of the orbit as derived by the usual method of linear error propagation. To describe the possible variation of these components in detail, however, the full covariance matrix must be taken into account. This has been done by calculating the semi-major-axis vectors of the corresponding six-dimensional error ellipsoid. Because the ellipsoid is highly flattened it is sufficiently characterized by the two largest vectors. By adding and subtracting them from the mean initial values, four typical sets of alternative initial values were produced and an orbit calculated for each of them. The results are documented in Table 7. They give an impression of how accurately the orbital parameters of M3 can in fact be determined. The accuracy of the values of the two constants of motion is shown in Fig. 10. Here linear error propagation had to be replaced by a more complicated pointwise error simulation to give the characteristic curves of 50, 66 and 90 per cent likelihood. Note that there remains some uncertainty about the sign of J_z (sense of rotation around the z-axis).

5 DISCUSSION

We have shown that it is possible to obtain the absolute proper motion of Galactic globular clusters directly with respect to a large number of background galaxies using Tautenburg Schmidt plates measured on the APM facility. In comparison with the results of Cudworth (1979) the epoch difference is only moderate and the accuracy in measuring the position of any individual object is much worse because of the smaller epoch difference and our much smaller plate scale. However, the advantages in being able to use a reference frame of thousands of background galaxies outweigh these drawbacks. Indeed, the reference frame can be established to an accuracy of less than ± 0.05 arcsec (100 yr)$^{-1}$. In

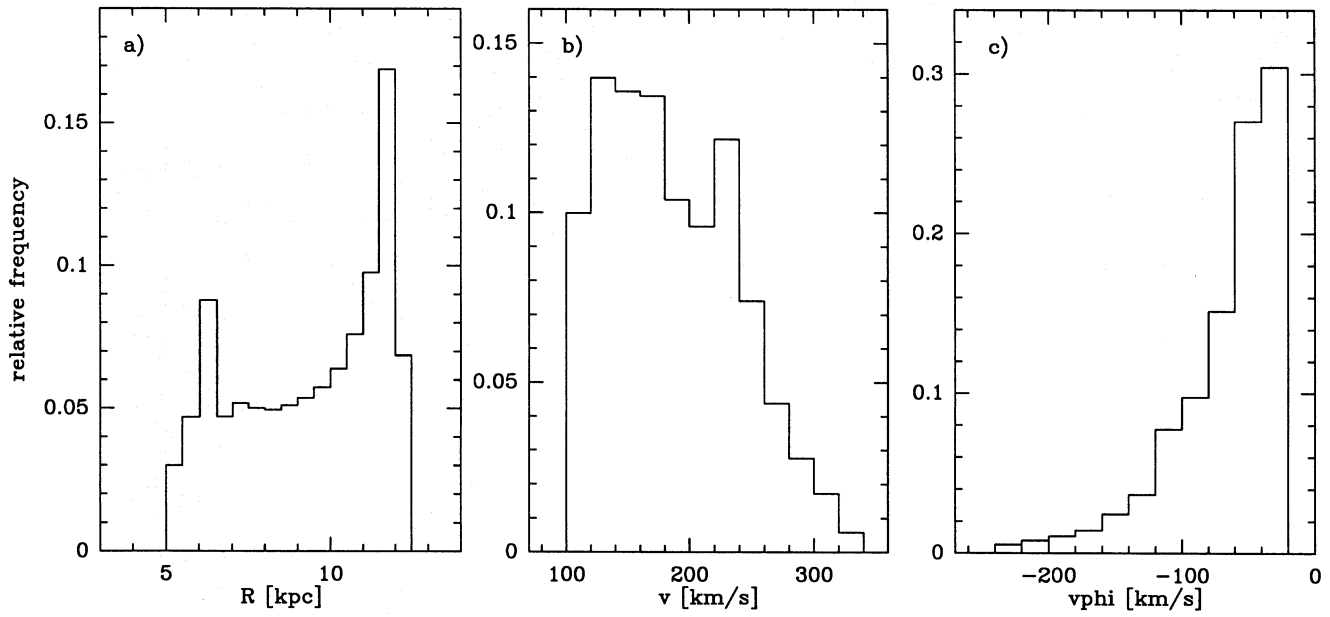

Figure 9. Distribution of values of selected orbital parameters along the orbit in the time interval (− 10; 0) Gyr.

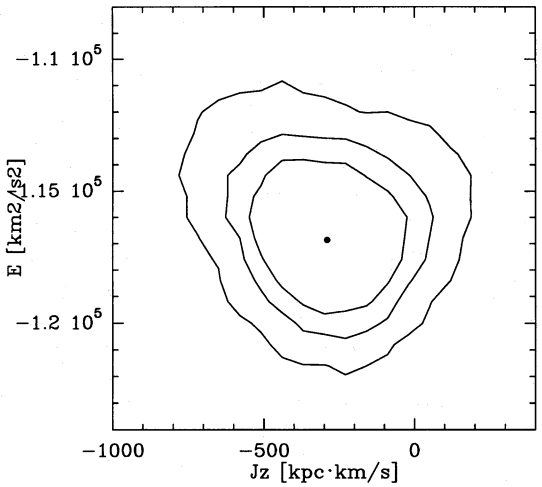

Figure 10. Uncertainty in the determination of the constants of motion. The point corresponds to the values of the mean orbit, and the lines refer to 50, 66 and 90 per cent likelihoods.

spite of the similar direction of the solar apex with respect to faint stars and the globular cluster system we find a significant difference between the field and cluster proper motions for stars of the same magnitude interval.

Using the results of our proper motion determination with respect to the well-defined extragalactic reference frame we can describe the space motion of the globular cluster very accurately. With some further assumptions on the motion of the Sun and on the Galactic model we obtain a kind of box orbit for M3. The space motion consists of rapidly precessing ellipses with oscillating eccentricity, and the cluster's distance from the Galactic Centre varies between 5 and 12 kpc. To give an impression of the accuracy of the orbital parameters of M3 the orbit determination was repeated using four alternative sets of initial values produced by taking into account the errors in the observations. No essential changes of the orbit were found.

In future work we intend to address the problem of determining the proper motions of some of the Galactic dwarf spheroidal satellites in addition to extending the work to other globular clusters to exploit fully all of the Tautenburg plate material.

ACKNOWLEDGMENTS

We wish to thank the Karl-Schwarzschild-Observatorium, Tautenburg, particularly Dr F. Börngen and Dr R. Ziener for supplying the plates, and Dr N. Argue of the Institute of Astronomy for his support during this project. RDS would like to thank the Institute of Astronomy, Cambridge for hospitality and financial support during some of this work. The APM is a national astronomy facility financed by the Science and Engineering Research Council. The WIP-Projekt Astrometrie bei der Universität Potsdam is supported by the Koordinierungs und Aufbau-Initiative für die Forschung.

REFERENCES

Allen C., Martos M. A., 1986, Rev. Mex. Astron. Astrofis., 13, 137
Bronkalla W., 1972, Dissertation, Potsdam
Brosche P., Geffert M., Ninkovic S., 1983, Publ. Astron. Inst. Czech. Acad. Sci., 56, 145
Brosche P., Geffert M., Klemola A. R., Ninkovic S., 1985, AJ, 90, 2033
Bunclark P. S., Irwin M. J., 1983, in Rolfe E. J., ed., Proc. Int. Colloq. on Statistical Methods in Astronomy, ESA SP-201. ESA Publications Division, Noordwijk, p. 195
Cudworth K. M., 1979, AJ, 84, 1312
Cudworth K. M., Hanson R. B., 1993, AJ, 105, 168
Evans D. W., 1988, PhD thesis, Univ. Cambridge
Gunn J. E., Griffin R. F., 1979, AJ, 84, 752
Hanson R. B., 1987, AJ, 94, 409
Hirte S., Dick W. R., Schilbach E., Scholz R.D., 1990, in Jaschek C., Murtagh F., eds, Proc. Conf. on Errors, Uncertainties and Bias in Astronomy. Cambridge Univ. Press, Cambridge, p. 343
Irwin M. J., 1985, MNRAS, 214, 575
Johnson D. R. H., Soderblom D. R., 1987, AJ, 93, 864
Kibblewhite E. J., Irwin M. J., Bridgeland M. T., Bunclark P. S., 1982, Occ. Rep. R. Obs. Edin., 10, 79
Kibblewhite E., Bridgeland M., Bunclark P., Cawson M., Irwin M., 1984, in Capaccioli M., ed., Proc. Conf. on Astronomy with Schmidt-Type Telescopes. Reidel, Dordrecht, p. 89
Klemola A. R., Vasilevskis S., 1971, Publ. Lick Obs., XXII, part III
Mihalas D., Binney J., 1981, Galactic Astronomy. Freeman, San Francisco
Odenkirchen M., Brosche P., 1992, Astron. Nachr., 313, 69
Paez E., 1990, A&AS, 84, 481
Röser B., Bastian U., 1988, A&AS, 74, 449
Schilbach E., 1982, Astron. Nachr., 303, 335
Schilbach E., Scholz R.-D., 1992, Astron. Nachr., 313, 243
Scholz R.-D., 1990, Dissertation (A), Potsdam
Scholz R.-D., Hirte S., 1991, Astron. Nachr., 312, 45
Scholz R.-D., Rybka S. P., 1988, Astron. Nachr., 309, 47
Scholz R.-D., Schmidt K.-H., 1992, Astron. Nachr., 313, 45
Tucholke H.-J., 1992a, A&AS, 93, 293
Tucholke H.-J., 1992b, A&AS, 93, 311
Webbink R. F., 1988, in Grindley J. E., Davis Philip A. G., eds, IAU Symp. 126, The Harlow Shapley Symposium on Globular Cluster systems in Galaxies. Kluwer, Dordrecht, p. 49